AguaClara Cornell Floc Modeling

Spring 2025: Mid-Semester Report

Anjali Asthagiri (aa2549), Isabel Crovella (isc25), Alex Gardocki (rag325), Lauren Hsu (lkh58), Max Zheng (hz687)

Mar 14, 2025

Abstract

Most surface water treatment plants, including AguaClara technology, rely on flocculation and clarification processes for particle aggregation and removal. This research project aims to develop a mathematical model of these processes that can be applied to optimize the design of treatment plants and reduce operating costs. There are two main focus areas for this project: investigating and predicting (I) floc filter dynamics during clarification and (II) particle collisions during flocculation. Specifically, the Spring 2025 Floc Modeling team aims to develop an understanding of the spatial distribution of floc saturation in the floc filter. The team is designing and conducting experiments with a miniature clarifier to visualize gradients in floc saturation within the floc filter, correlate floc filter saturation state with primary particle removal performance, and analyze how influent turbidity and coagulant dose conditions affect floc saturation. To further develop the flocculation model, the team is introducing new mechanisms to the model, including coagulant attachment to the flocculator walls and coagulant attachment to other coagulant nanoparticles. The improved flocculation and clarification models will be applied to automate coagulant dosing in collaboration with the Automated Coagulant Dosing Controller (ACDC) subteam.

Introduction

Effective water treatment is essential for public health and the welfare of communities. Untreated water typically contains small primary particles made of silt, clay, and sand (<1 μm diameter) and dissolved organic matter (DOM) such as plant and animal material, algae, and bacteria. In the AguaClara treatment process, flocculation and clarification processes are critical, as they remove most of these particles before filtration and chlorination. While these processes are widely used throughout the water treatment industry, gaps remain in our understanding of their underlying physical mechanisms. This lack of understanding has made it challenging to optimize the design of treatment plants and develop automated systems that can successfully respond to fluctuating conditions. As a result, water treatment facilities may experience inefficiencies that not only reduce performance, but also result in high operational costs.

The framework of AguaClara's current understanding of flocculation and clarification is as follows. Flocculation combines primary particles into larger aggregates called flocs (10-500 μm diameter), which can more easily be removed through gravity-driven sedimentation. For flocs to form successfully, a coagulant particle must be present at the point of contact since it

enables covalent bonding between clay particles and is therefore necessary for successful clay-clay attachment. Hence, a sufficient amount of coagulant must be added prior to flocculation for this process to be effective. However, adding too much coagulant is wasteful and overdosing failures have been observed.

Clarification follows flocculation. It is a process that allows the newly formed flocs to settle and separate from the treated water. During conventional clarification, flocs settle and are wasted. In order to increase the efficiency of clarification, AguaClara plants utilize a process called floc sweeping, where previously formed flocs capture additional primary particles in a suspension called a floc filter. Water jets maintain the water flow in the floc filter and guide smaller flocs through the floc filter and towards the plate settlers. These angled plates help smaller flocs aggregate further and eventually settle back into the floc filter.

Floc sweeping efficiency depends on coagulant dose, floc filter concentration, and floc saturation. As a floc captures primary particles, its pores fill. Once the floc is fully saturated, it cannot capture additional particles. Spatial variations in floc saturation within the clarifier can affect particle removal efficiency in the clarifier.

While the processes of flocculation and clarification are fundamental to water treatment, they are also complex, with many underlying mechanisms still not fully understood. The interactions between coagulant dose, floc formation, and particle capture involve a range of physical and chemical variables that make it difficult to predict and optimize performance. A mathematical model is essential for addressing these uncertainties, particularly in three key areas: (1) automating coagulant dosing, (2) optimizing clarifier design by managing floc saturation, and (3) improving flocculator design to enhance particle aggregation. An effective model must be both accurate and simple as it ensures that the model can be applied in real-world settings to inform design decisions and automate treatment processes. Current models, however, require further refinement to achieve this goal, as will be discussed in the Literature Review section below.

Literature Review & Previous Work

Flocculation Modeling with Charge Neutralization Theory

The successes and failures of past flocculation models must be considered in order to investigate the mechanisms of flocculation. To understand how to model flocculation, the first mechanism to consider is coagulant function. The coagulant used for experimentation, Poly-Aluminum Chloride (PACl), forms sticky hydroxide nanoparticles in the solid phase when diluted with water as seen in Equation 1.

$$[Al_n(OH)_mCl_{3n-m}]_x + H_2O \rightarrow Al(OH)_3 \text{ (or } Al_{13}O_4(OH)_{24}^{2+}) + H^+ \qquad \text{Equation 1}$$

Previous flocculation models are based on Charge Neutralization Theory (CNT) or DLVO Theory, which explain why there is an optimal coagulant dosage for a certain amount of charged particles present in untreated water (Runkana 2004). The theory explains that the

amount of charge contributed by the positive metal cation Al^{3+} effectively neutralizes the negative charges of the clay primary particles, allowing them to join together and eventually form flocs under appropriate collision conditions.

Figure 1a demonstrates the electrical double layer (EDL), measured by the Nernst potential. Constituted by the Stern potential and the zeta potential, the Nernst potential is a measure of the total electrical potential at the surface of a particle. Due to charged particles wanting to achieve electrical neutrality, positive ions from the solution group around the negatively-charged primary particle to form the Stern layer. The Stern layer directly contributes to the Stern Potential, which is the decrease in the electric potential of the primary particle due to the gathering of positive charges in the Stern layer.

As more coagulant is added, the Stern layer increases in charge, decreasing the Zeta potential and compressing the EDL by making the initial electrostatic potential gradient much steeper. The Zeta potential represents the repulsive force from the primary particle, and so as it decreases, the probability of collision between two primary particles with low Zeta potentials increases. This idea is demonstrated by the unstable system seen in Figure 1b, which is preferable for flocculation compared to the stable system. The unstable system has a lower resultant force as a function of the distance between two primary particles, and so they are more likely to collide and aggregate.

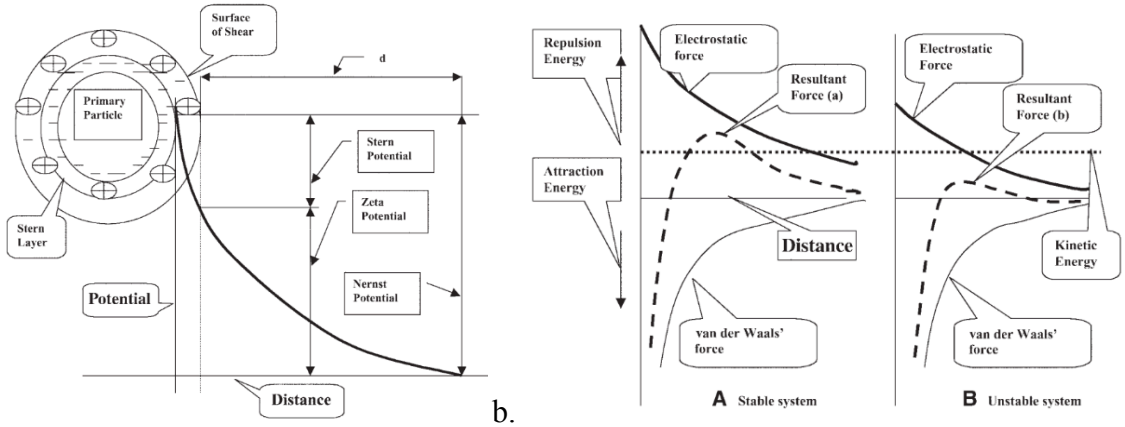

Figure 1. From Shammas, Nazih K. demonstrating (a) the electrical potential of a negatively charged colloidal particle, and (b) the effect of interparticle forces on the stability of a colloidal system. (2005)

While CNT is correct in its beliefs that the addition of coagulant helps to compress the EDL and lower the zeta potential, it fails to fully meet a few observed flocculation tendencies. For example, at high turbidities, lower dosages of coagulants relative to turbidity work just as effectively compared to low turbidities despite a measure of the zeta potential not indicating full neutralization of charges or a stoichiometric relationship. Instead, Chen et al. (2006) demonstrated that when dosed linearly with turbidity, observations such as the formation of smaller flocs indicate an overdosing failure, resulting in a destabilization of the floc filter.

Another oversight of the CNT stems from its assumptions about coagulant functionality. Since the CNT believes coagulant only contributes charge neutralization, it leads to the conclusion that once two primary particles overcome their EDLs, the bonds holding together particles are simply intermolecular van der Waals forces. However, this cannot be true as throughout the flocculation process, aggregations of particles experience forces much higher than van der Waals forces. According to Swetland et al., this means flocculation would cause particles to separate after aggregation under CNT, despite flocculation being the primary reason for particle aggregation (2014). The last observation CNT fails to explain is the formation of coagulant flocs in deionized water. Without any clay or other floc-forming particles present, the injection of pure coagulant still leads to the observed formation of flocs which are theorized to be comprised of coagulant-coagulant bonds by Swetland et al. (2013).

These shortcomings of the CNT lead to the hypothesis that Charge Neutralization Theory is not capable of fully explaining the formation of flocs due to coagulant. This shifted the focus of flocculation modeling towards collision-based models, where flocculation is driven by the frequency and attachment efficiency of particle collisions rather than the charge of the particles.

Flocculation Modeling with a Collision-Based Approach

The flocculation model developed by Argaman and Kaufman (1970) offers a conceptual basis for describing the competition between particle aggregation and floc breakage. However, the model is constrained by several assumptions that limit its accuracy and applicability. The model tracked the concentration of primary particles, which cannot be directly measured, and assumed that particle movement is governed by large-scale eddies and that small particles collide with larger aggregates. These assumptions were later refuted by Casson and Lawler (1990), who showed that collisions are primarily driven by small-scale eddies and typically occur between particles of similar sizes. Additionally, Argaman and Kaufman (1970) and Liu et al. (2004) demonstrated that floc breakup has a negligible role compared to aggregation, further undermining the model's premise. The practical application of the model is also limited by its reliance on empirical constants, which are influenced by influent turbidity and coagulant dosage (Haarhoff & Joubert, 1997).

Lee et al. (2000) and Casson and Lawler (1990) applied the Smoluchowski (1917) model to describe particle distribution during flocculation, relying on parameters for collision frequency and efficiency. Although this approach introduced a more granular perspective on particle interactions, it required simplifying assumptions to render the equations usable. The parameters are highly system-specific and do not account for critical physical and mechanistic factors, reducing the adaptability of the model to varying conditions.

More recently, computational fluid dynamics (CFD)-based approaches have modeled spatial velocity gradients. Studies have shown that extreme gradients, rather than average values, dominate floc breakage, making spatially-resolved CFD models particularly valuable (Bridgeman et al., 2009). Nevertheless, CFD models are computationally intensive and often impractical for exploring a wide range of design conditions.

The mechanistic model introduced by Pennock et al. (2018) and Du et al. (2019) presents a promising advancement. This model describes the transformation of non-settleable particles into settleable flocs—a measurable quantity—and depends primarily on physical rather than empirical constants, making it more adaptable. Du et al. (2019) expanded the model to consider the influence of dissolved organic matter on collision efficiency. While the model has demonstrated practical value, particularly for informing flocculator design and predicting settled turbidity, discrepancies with experimental findings have been observed (Tse et al., 2011). The model may be limited by not accounting for coagulant-coagulant and coagulant-wall collisions, the relative strengths of coagulant-coagulant and coagulant-clay bond strengths, and the finite strength of particle bonds at the time of collision. Therefore this study will focus on expanding the model to include these mechanisms in order to enhance the predictive accuracy of the model.

Clarification Modeling

Vitasovic (1986) and Takacs et al. (1991) developed a 1D model of clarification based on solids flux theory to predict the sludge blanket settling velocity. The Takacs model unified the description of both discrete and hindered settling into a single equation. However, Gernaey et al. (2001) highlighted the difficulty of fitting this model, limiting its utility in practical applications. Head et al. (1997) modeled floc blanket clarification by examining how influent concentration and floc wastage flow rate influence the height and concentration of the floc blanket. However, the model is limited in its ability to describe how particle size distribution post-flocculation and coagulant dosage impact clarification performance.

Sarmiento (2021) addressed this gap by applying the Pennock et al. (2018) flocculation model which accounts for coagulant dosage and distinguishes between the settleable and non-settleable particles formed during flocculation. Sarmiento (2021) assumes that all settleable particles generated during flocculation are removed during clarification. In contrast to model predictions, experimental results indicate that clarification performance decreases over time, possibly due to effects of floc saturation. Pennock et al. (2024) modified the Pennock et al. (2018) flocculation model to describe how the conversion from non-settleable to settleable particles depends on clarifier design. Nonetheless, their work did not incorporate floc sweeping and floc saturation, which are of significance in floc filter-based clarifiers. In the summer of 2024, our team built on these models to account for floc sweeping and floc saturation. Despite these enhancements, discrepancies between experimental and theoretical parameter values exist, indicating the need to reevaluate the assumptions of the model (Appendix Section I). The major assumptions are that flocs in the floc filter are at their steady-state saturation level and the floc filter is well-mixed. Therefore experimentation is needed to investigate the spatial and temporal dynamics of the floc filter. This semester, the subteam is specifically focused on understanding the dynamics of floc saturation within the clarifier.

Methods

Part I: Floc Saturation Experiments

Experimental Setup

In order to experimentally guide our development of models for flocculation and clarification, and specifically to investigate floc saturation within the floc filter, we designed a small-scale, low-hydraulic residence time clarifier to allow for a novel approach to visualizing floc saturation. In the experimental setup, a white clay stock solution and coagulant first flows through a tube flocculator. After exiting the flocculator, a red kaolin clay stock solution is added to the stream and pumped into the clarifier. This serves to add colored primary particles to the clarifier influent. Within the clarifier, the flocs formed from the white clay and coagulant settle to form a floc filter that captures the red clay primary particles through floc sweeping. Excess flocs overflow into the floc hopper to be drained. A set of plate settlers provides additional surface area to aggregate small flocs and reintroduce them to the floc filter. Effluent exits above the plate settlers.

In this setup, the coloration of the floc filter may provide insights into the spatial distribution of floc saturation. Capturing additional primary particles increases the saturation of a floc, so flocs which have captured more of the red clay primary particles will be more saturated. Hence, a region having a stronger coloration relative to the rest of the floc filter may indicate that the flocs in that region are more highly saturated.

When designing our miniature clarifier, we attempted to capture the characteristics of a full size AguaClara plant while allowing for modifications to test different conditions. For example, the diffuser inlet uses a threaded adapter which screws into the clarifier. Since this inlet adapter is resin-printed, new adapters with different sizes and diffuser shapes can be printed easily, giving us control over influent velocity and the initial velocity gradient in the clarifier. The current diffuser inlet widens outward so that the influent velocity is consistent between cross-sections parallel to the viewing plane. To prevent interference with the floc filter, rather than being directed downward toward the jet reverser, the jet enters from the side and is redirected 90º by the jet reverser, which is shaped as a quarter circle. The angle of the diffuser is 50º, consistent with AguaClara plants (Weber-Shirk, n.d.). The height of the floc filter is 134 mm.

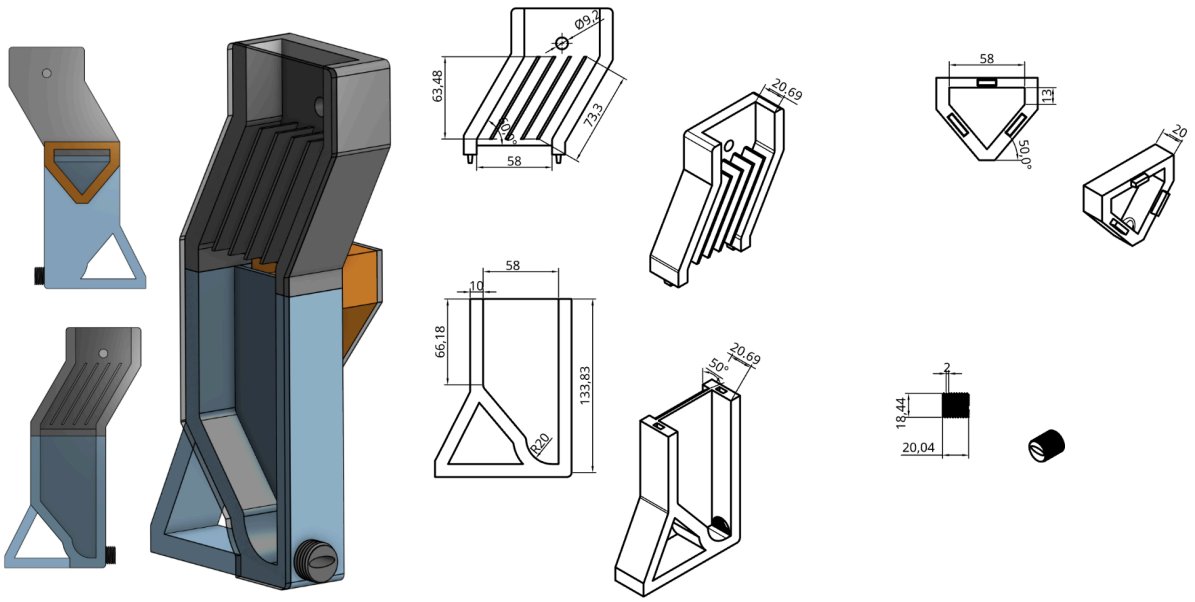

Figure 2. Clarifier schematic. Dimensions are in millimeters.

For the upflow velocity, 1 mm/s was chosen based on the specifications for AguaClara plants (Weber-Shirk, n.d.). Given the targeted flow rate of 1.2 mL/s based on the Dissolved Organic Matter (DOM) subteam's prior work with the tube flocculator, the cross-sectional area of the clarifier was designed to be 1200 mm^2. An initial influent velocity of 21 mm/s through the diffuser was chosen in order to have sufficient speed to keep the floc filter suspended. To achieve this, a cross sectional area of 57.55 mm^2 was chosen for the diffuser inlet.

For the plate settlers, a spacing of 1 cm between plates was chosen to avoid floc rollup. Using the equation found in the AguaClara textbook (Weber-Shirk, n.d.), we calculated the necessary plate settler length to be 14.667 cm to ensure the AguaClara standard capture velocity of 0.12 mm/s. However, due to limitations in print size, we chose to reduce the length to 7.33 cm, resulting in a capture velocity of 0.73 mm/s. A plate width of 2.0 mm was chosen to balance the integrity of the print with having the thinnest plates possible to reduce the increase in upflow velocity through the plate settlers. The plates were placed at a 60º angle based on AguaClara clarifier specifications (Weber-Shirk, n.d.). The area above the plate settlers was left open to the air to prevent air bubbles from being trapped in a closed system.

Lastly, we added a floc weir connected to a floc hopper in order to remove excess flocs from the floc filter. We utilized the same clear acrylic on the hopper as the front of the clarifier in order to visualize when the floc hopper must be emptied. Pumps are used to remove waste from the floc hopper and effluent from the top of the clarifier.

Experimental Design

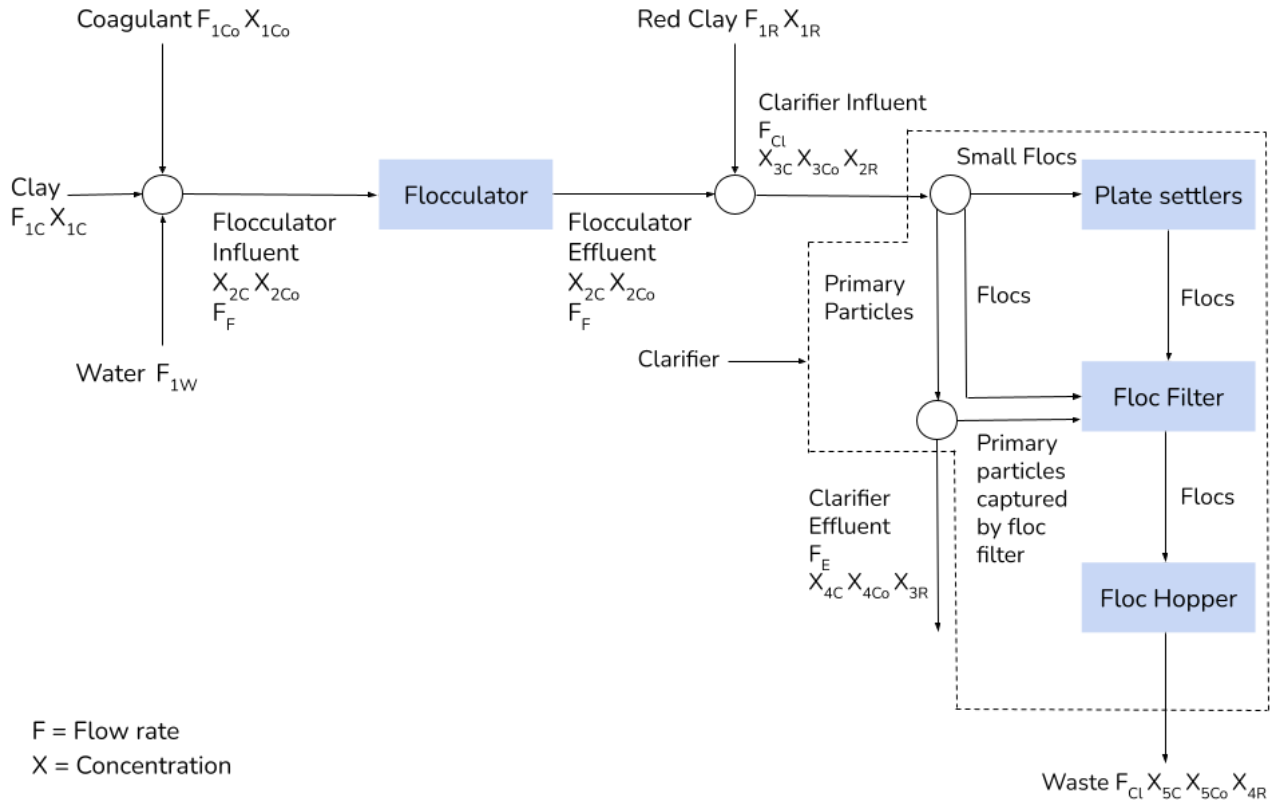

Figure 3. Process flow diagram illustrating movement of clay, coagulant, and red clay through the experimental setup.

Figure 4. Picture of experimental setup in lab. The clarifier is seen mounted on the bottom left.

A mass balance calculator was created to determine flow rates and pump speeds in the experimental setup shown in Figure 3. The mass balance calculator takes inputs for stock concentrations and clarifier influent concentrations of coagulant, clay, and red clay and the flow rate of the waste pump. Flow rates are calculated using the total clarifier influent flow rate (1.2 mL/s), stock concentration, and target clarifier influent concentration. Pump speeds are then determined using the flow rates and volume per revolution for each pump. See Appendix II for mass balance calculations.

For all experiments, the floc filter will be grown rapidly in the clarifier with a higher influent turbidity and coagulant dosage, before transitioning to standard influent and coagulant conditions and adding red clay. The expected time to grow a floc filter is 29.33 minutes, which was calculated using Equation 2.

$$Floc\ filter\ growth\ time\ = \frac{A_{\ Clarifier\ cross-sectional\ area} \times H_{\ Floc\ filter\ height} \times T_{\ Theoretical\ floc\ filter\ concentration}}{F_{\ Total\ clarifier\ influent\ flow\ rate} \times C_{\ Clay\ clarifier\ influent\ concentration}} \qquad \text{Equation 2}$$

Initial Experiments

One experiment was run in order to test the rapid growth of a floc filter. The clay stock solution was pumped into the clarifier at 49.07 rev/s and the coagulant stock solution was pumped at 91.82 rev/s to reach influent concentrations of 100 mg/L and 30 mg/L respectively. An effluent pump was used to prevent the clarifier from overflowing and was run at 0.43 rev/s to

match the influent flow rate of 1.2 mL/s. The experiment was run for 30-45 minutes and successfully formed white flocs and maintained a suspended floc filter.

Figure 5. Initial experiment forms a floc filter in the clarifier.

The goal of the next experiment is to verify that red clay can be used to model primary particle capture by varying the influent concentration of red clay. Following the growth of the floc filter, the coagulant and white clay streams will be stopped, while the clarifier influent concentration of red clay will be set at 50 NTU. After an hour, only water will be flowed through the system for 45 minutes and the coloration of the floc filter will be visualized.

Appendix

Section I: Current Clarification Model

Currently, it is defined that

(2)

$$C_{clarified} = C_{flocculated} e^{-k_c \frac{C_{coagulant}}{C_{influent}} (1 - P_{floc\ saturated})^{2/3} h_{floc\ filter}} \quad where\ k_C = k' \beta \frac{\pi r^2_{floc} C_{floc\ filter}}{m_{floc}}$$

(3)

$$C_{flocculated} = \left(\frac{C_{coagulant}}{k_{pf} C_{influent}} + C_{influent}^{-2/3} \right)^{-3/2} \text{ where } k_{pf} = \frac{3}{2\pi k k' G \theta} \left(\rho \frac{\pi}{6} \right)^{2/3}$$

$$P_{floc\ saturated} = \frac{C_{flocculated} - C_{clarified}}{q(C_{influent} - C_{clarified})} \quad (4)$$

$$C_{coagulant} = C_{coagulant\ added} - \lambda C_{DOM} \quad (5)$$

where λ, k, k', and β are proportionality constants, G is the mean velocity gradient in the flocculator, ϱ is the density of clay primary particles, θ is the flocculation residence time, and q is the maximum total mass of primary particles collected per floc in the floc filter.

The value of the constant, k_c , (see equation 2) suggests there is a critical component missing from this clarification model. When fitting the model to AguaClara plant data from La Concordia Nicaragua, the fitted and theoretical values of k_c are orders of magnitude off—with 0.0016 as the theoretical value and 1000 as the fitted value.

Section II: Mass Balance Calculations for Experimentation

Total clarifier influent flow rate (mL/s)	1.2
Effluent flow rate (mL/s)	1.2
Clay/coagulant/red clay clarifier influent flow rate (mL/s)	x
Clay/coagulant/red clay flocculator influent concentration (M)	i
Clay/coagulant/red clay clarifier influent concentration (M)	c
Clay/coagulant/red clay stock concentration (M)	s
Clay/coagulant/red clay pump volume per revolution (mL/rev)	n
Clay/coagulant/red clay pump speed (rev/s)	v
Total flocculator influent flow rate (mL/s)	f
Water flow rate (mL/s)	w
Waste flow rate (mL/s)	a
Effluent with wasting flow rate (mL/s)	e

The equations below found the flow rates and pump speeds during the experiment.

$$x = \frac{1.2\,c}{s}$$
$$v = \frac{60\,x}{n}$$
$$f = 1.2 - w$$
$$i = \frac{sx}{f}$$
$$e = 1.2 - a$$

Section III: Apparatus Specifications

PUMPS

Name	ID	Tubing Size	Volume per Rev (mL/rev)
Clay	2	2mm	0.112866
Water	3	17 (6.4mm ID) (# MasterFlex 06508-17)	2.66327
Rose Clay	9	1.65mm	0.0259664
Coagulant	1	2mm	0.117623
Waste	5	16 (⅛'' ID) (# MasterFlex 06508-16)	0.849814
Effluent	8	17 (6.4mm ID) (# MasterFlex 06508-17)	2.785

TURBIDIMETERS

Name	ID
Influent	7
Clarified	6

Figure A1. Pump and turbidimeter specifications. The volumes per revolution were determined manually.

References

Argaman, Y., & Kaufman, W. J. (1970). Turbulence and flocculation. *Journal of the Sanitary Engineering Division*, *96*(2), 223–241. https://doi.org/10.1061/jsedai.0001073

Bridgeman, J., Jefferson, B., & Parsons, S. A. (2009). Computational Fluid Dynamics Modelling of Flocculation in Water Treatment: A review. *Engineering Applications of Computational Fluid Mechanics*, *3*(2), 220–241. https://doi.org/10.1080/19942060.2009.11015267

Casson, L.W. and Lawler, D.F. (1990) Flocculation in Turbulent Flow: Measurement and Modeling of Particle Size Distributions. J. *American Water Works Association*, 82, 54-68.

Chen, L. C., Lee, D. J., Chou, S. S. (2006). Charge Reversal Effect on Blanket in Full-Scale Floc

Blanket Clarifier. *Journal of Environmental Engineering, 132*(11). https://doi.org/10.1061/(ASCE)0733-9372(2006)132:11(1523)

Du, Y., Pennock, W. H., Weber-Shirk, M. L., & Lion, L. W. (2019). Observations and a geometric explanation of effects of humic acid on flocculation. *Environmental Engineering Science*, *36*(5), 614–622. https://doi.org/10.1089/ees.2018.0405

Gernaey, K., Vanrolleghem, P. A., & Lessard, P. (2001). Modeling of a reactive primary clarifier. *Water Science & Technology*, *43*(7), 73–81. https://doi.org/10.2166/wst.2001.0393

Haarhoff, J., & Joubert, H. (1997). Determination of aggregation and breakup constants during flocculation. *Water Science & Technology*, *36*(4). https://doi.org/10.1016/s0273-1223(97)00416-2

Head, R., Hart, J., & Graham, N. (1997). Simulating the effect of blanket characteristics on the floc blanket clarification process. *Water Science & Technology*, *36*(4). https://doi.org/10.1016/s0273-1223(97)00422-8

Liu, J., Crapper, M., & McConnachie, G. (2004). An accurate approach to the design of channel hydraulic flocculators. *Water Research*, *38*(4), 875–886. https://doi.org/10.1016/j.watres.2003.10.014

Pennock, W. H., Weber-Shirk, M. L., & Lion, L. W. (2018). A hydrodynamic and surface coverage model capable of predicting settled effluent turbidity subsequent to hydraulic flocculation. *Environmental Engineering Science*, *35*(12), 1273–1285. https://doi.org/10.1089/ees.2017.0332

Runkana, V., Somasundaran, P., & Kapur, P. C. (2004). Mathematical modeling of polymer-induced flocculation by charge neutralization. *Journal of Colloid and Interface Science, 270*(2), 347-358. https://doi.org/10.1016/j.jcis.2003.08.076

Sarmiento, K. (2021). Particle Removal in Floc Blanket Clarifiers Via Internal Flow Through Porous Fractal Aggregates. *Cornell University*.

Shammas, N.K. (2005). Coagulation and Flocculation. In: Wang, L.K., Hung, YT., Shammas, N.K. (eds) Physicochemical Treatment Processes. *Handbook of Environmental Engineering, 3*(103-139). Humana Press. https://doi.org/10.1385/1-59259-820-x:103

Smoluchowski, M. (1917) Mathematical Theory of the Kinetics of the Coagulation of Colloidal Solutions. *Zeitschrift für Physikalische Chemie*, 19, 129-135.

Swetland, K. A., Weber-Shirk, M. L., Lion, L. W. (2013). Influence of Polymeric Aluminum Oxyhydroxide Precipitate-Aggregation on Flocculation Performance. *Environmental Engineering Science, 30*(9). https://doi.org/10.1089/ees.2012.0199

Swetland, K. A., Weber-Shirk, M. L., Lion, L. W. (2014). Flocculation-Sedimentation

Performance Model for Laminar-Flow Hydraulic Flocculation with Polyaluminum Chloride and Aluminum Sulfate Coagulants. *Journal of Environmental Engineering, 140*(3). https://doi.org/10.1061/(ASCE)EE.1943-7870.0000814

Takács, I., Patry, G., & Nolasco, D. (1991). A dynamic model of the clarification-thickening process. *Water Research*, *25*(10), 1263–1271. https://doi.org/10.1016/0043-1354(91)90066-y

Tse, I. C., Swetland, K., Weber-Shirk, M. L., & Lion, L. W. (2011). Fluid shear influences on the performance of hydraulic flocculation systems. *Water Research*, *45*(17), 5412–5418. https://doi.org/10.1016/j.watres.2011.07.040

Vitasovic, Z. Z. (1986). An Integrated Control Strategy for the Activated Sludge Process. Rice University.

Weber-Shirk, M. (n.d.). Clarification Introduction. *The Physics Of Water Treatment Design.* https://aguaclara.github.io/Textbook/Clarification/Clarifier_Intro.html